CONFERENCE PRE-PRINT

FREQUENCY HYSTERESIS OF MHD INSTABILITIES IN HELICAL AND TOKAMAK PLASMAS

Y. TAKEMURA National Institute for Fusion Science Toki, Japan Email: takemura.yuki@nifs.ac.jp

K. WATANABE National Institute for Fusion Science Toki, Japan

A. ISAYAMA National Institutes for Quantum Science and Technology Naka, Japan

G. MATSUNAGA National Institutes for Quantum Science and Technology Naka, Japan

Y. SHIBATA National Institute of Technology, Gifu College Gifu, Japan

Abstract

The relationship between the amplitude and frequency of magnetic fluctuations driven by MHD instabilities in toroidal magnetically confined plasmas has been investigated. In LHD and JT-60U, it has previously been observed that, prior to mode locking, the amplitude—frequency relationship follows a unique trajectory, which can be reproduced by the force balance model between the electromagnetic braking force and the viscous driving force. In contrast, new phenomena have been observed in which the trajectory differs between the frequency-decreasing and frequency-increasing phases, which cannot be explained by the conventional model. Furthermore, in LHD, a new behaviour was observed in which the lower limit of the frequency after the decrease is restricted to approximately half of its pre-decrease value. These new behaviours have been successfully explained by an extended model that incorporates the combination of the two braking models and taking into account the deviation of the magnetic fluctuation frequency from the plasma flow.

1. INTRODUCTION

In magnetically confined toroidal plasmas, following a decrease in the frequency of magnetic fluctuations due to MHD instabilities, an increase in fluctuation amplitude can occur, leading to confinement degradation. In particular, when the frequency of magnetic fluctuations decreases nearly to zero, the instability grows (referred to as a locked mode[1,2]) and may even trigger a disruption. Therefore, a method of stabilizing NTMs with ECH/ECCD before mode locking[3] and a method of re-rotation from mode locking using rotating RMPs[4] have been demonstrated, and an increase in the instability frequency has been observed during the stabilization. Therefore, from the perspective of instability control, it is important not only to understand the MHD behaviour during frequency decrease but also during frequency increase, as well as to predict such behaviour in future devices.

The characteristic behaviour of mode frequency increase and decrease before the mode locking has been observed in locked-mode discharges in LHD[5] and in neoclassical tearing mode discharges with applied ECCD in JT-60U[6]. In both cases, the trajectory in the amplitude–frequency diagram remains unique during both phases. This behaviour is well explained by the force balance model, which captures the balance between a decelerating electromagnetic force and an accelerating viscous force[7]. In the case of locked-mode discharges in LHD, the main electromagnetic force is the interaction between the perturbed current driven by the instability and the plasma response field induced by the externally applied RMPs from the RMP coils ($F_{\rm RMP}$). Whereas in NTM discharges of the JT-60U, it is attributed to the interaction between the instability-driven perturbed current and the associated eddy-current-driven magnetic perturbation ($F_{\rm rw}$).

This study reports observations of different MHD behaviours during frequency deceleration and acceleration in the JT-60U tokamak and the LHD stellarator, which cannot be explained by conventional models. An extended model is introduced, which successfully explains these new experimental observations. The present proceedings are organized as follows. Section 2 presents new experimental observations from JT-60U and introduces the extended model to explain them. Section 3 provides a comparison between the observations in LHD and the modelling results, and finally, Section 4 presents the summary and discussion.

HYSTERISIS DURING FREOUENCY DECELERATION AND ACCELERATION IN JT-60U

In JT-60U, the amplitude–frequency trajectory of magnetic fluctuations driven by the NTM following the RWM revealed distinct MHD behaviours between the frequency deceleration and acceleration phases. The plasma current is 0.9 MA and the operational field is 1.5 T. The NBI heating power is maintained constant at approximately 16 MW, and the normalized beta is around 2.4. Figure 1 shows the time evolution of amplitude and frequency of m/n=2/1 magnetic fluctuation measured by saddle loops. The blue symbols indicate the data during the frequency-increasing phase, whereas the red symbols correspond to the frequency-decreasing phase. At around 6.0 s, a resistive wall mode (RWM) appears, followed by the excitation of an NTM at 6.2 s, during which the rotation frequency increases. At about 6.8 s, the frequency decreases nearly to zero, leading to mode locking, although no disruption is observed. Subsequently, the mode resumes rotation around 7.0 s. This rerotation may be attributed to the destabilization of the NTM due to the frequency decrease, which causes magnetic island growth, followed by a reduction in beta and the consequent stabilization of the NTM.

Figure 2 shows the trajectory of the amplitude and frequency corresponding to the data shown in the hatched area of Fig. 1. The blue symbols indicate phases of frequency increase, whereas the red symbols correspond to phases of frequency decrease. During the frequency-decreasing phase, the frequency drops abruptly from around 1500 Hz to almost zero, which is characteristic of a typical locked mode. In contrast, during the frequencyincreasing phase, the frequency rises gradually. In previous studies, the δb -f trajectory in the relatively highfrequency range (3-6 kHz) exhibited gradual frequency variations during both frequency increase and decrease. In contrast, the present study newly demonstrates that in the relatively low-frequency range, a frequency jump occurs during the frequency-decreasing phase.

In previous studies, the δb -f relationship was explained by a balance model between viscous driving torque and electromagnetic braking torque. The driving force and braking force are defined by the following equation. $F_{\rm D} \equiv \mu(\omega_0 - \omega) \quad (1), \\ F_{\rm B} \equiv \delta b_{\rm inst.} \times \delta b_{\rm inst.} \frac{\omega \tau_{\rm v}}{1 + \omega^2 \tau_{\rm v}^2} (2),$

$$F_{\rm D} \equiv \mu(\omega_0 - \omega) \quad (1),$$

$$F_{\rm B} \equiv \delta b_{\rm inst.} \times \delta b_{\rm inst.} \frac{\omega \tau_{\rm v}}{1 + \omega^2 \tau_{\rm v}^2} (2)$$

where $\delta b_{\text{inst.}}$ is the mode amplitude, τ_{v} is the wall constant time, and ω is the mode frequency. In this case, ω_0 is taken from the measured rotation frequency of the instability prior to the frequency decrease. Figure 3(b) illustrates a conceptual diagram of the balance model between braking force F_B (Eq. 2) and the driving force F_D (Eq. 1). The quasi-stationary frequency is evaluated from the intersection of the two. For example, when the magnetic fluctuation amplitude increases, the braking force becomes larger, and the intersection shifts gradually toward the lower-frequency region. However, in the region where ω_0 is small, three solutions exist. When the magnetic fluctuation amplitude increases in this regime, the solution shifts from three roots to a single root in the lowfrequency region. This transition corresponds to the frequency jump. The $F_{\rm rw}$ model is shown by the red curve in Fig. 2 and is in good agreement with the experimental observations, which supports the validity of the conventional F_{rw} model. However, since the eddy currents induced by the instability diminish as the mode frequency decreases, their influence becomes negligible in the low-frequency regime, such as that observed during the frequency-increasing phase, where the braking force is considered to be dominated by another perturbed magnetic field.

The frequency dependence of the plasma response field that provides the braking force is known to depend on the relative velocity between plasma rotation and the external magnetic field [7]. Since F_{rw} corresponds to the perturbed magnetic field driven by eddy currents induced by the instability, the relative velocity is nearly zero. In contrast, in the case of an external magnetic field with a large relative velocity, the frequency dependence of the

plasma response field changes, and the braking force is expressed as follows:
$$F_{\rm B} \equiv \delta b_{\rm inst.} \times \delta b_{\rm ext} \frac{\omega \tau_{\rm v}}{\sqrt{1 + \omega^2 \tau_{\rm v}^2}} \tag{3}.$$

Here, δb_{ext} denotes he plasma response field to the external magnetic field induced by certain factors. The conceptual diagram for this case is shown in Fig. 3(a). In this situation, no bifurcation occurs, and both frequency and amplitude always vary smoothly. The case with a large relative velocity is hereafter referred to as the slip condition, while the case with a small relative velocity is referred to as the no-slip condition. The slip model, shown by the blue curve in Fig. 2, successfully reproduces the observed gradual frequency variation. It should be emphasized that the same model parameters, τ_v and f_0 , are used for both the deceleration and acceleration phases. Moreover, the value of τ_v is 10 ms, which is found to be in good agreement with the wall time constant previously evaluated in earlier studies[8]. The combined slip and no-slip extended model successfully reproduces the hysteresis behavior.

3. HYSTERISIS DURING FREQUENCY DECELERATION AND ACCELERATION IN LHD

Different MHD activities during frequency acceleration and deceleration phases are observed in discharges of the instability with m/n=1/1 magnetic island ("Edge" MHD instability) observed in a relatively high-density regime of LHD[9]. The magnetic-axis major radius is 3.75 m, the operating magnetic field is 0.75 T, and the plasma aspect ratio is 6.3. The plasma is produced and sustained by tangential neutral beam injection (NBI); with hydrogen gas puffing, the line-averaged electron density reaches $\sim 4 \times 10^{19}$ m⁻³. The absolute value of plasma current is less than 10 kA/T, and the error field is corrected by externally applied RMPs.

Figure 4 shows the trajectory of the amplitude and frequency of the m/n=1/1 magnetic fluctuation in frequency-decreasing and increasing phases. Red and blue symbols represent observation during the frequency decrease and increase phases, respectively. During the frequency deceleration phase, the mode frequency gradually decreases in association with the growth of magnetic fluctuation amplitude. The lower limit reached after the frequency decrease differs from that in typical locked modes. Although in typical locked mode, the mode frequency falls to nearly zero, in this discharge, it decreases only to about half of its pre-decrease value; accordingly, no mode locking occurs. In discharges exhibiting locked-mode-like instabilities, re-rotation after mode locking has not been observed. In contrast, in the present discharge, an increase in frequency is observed following the frequency decrease. During the frequency-increasing phase, the mode follows a trajectory different from that of the decreasing phase. The hysteresis behaviour of instability was discovered in the amplitude-frequency trajectory during the frequency deceleration and acceleration phases.

According to previous studies in LHD, the perturbed magnetic field that provides the main braking force is the plasma response field induced by the external coil field. As mentioned above, this plasma response field is also considered in terms of slip and no-slip conditions. The expressions for the no-slip model and the slip model are presented below, respectively.

$$\begin{split} F_{\rm B} &\equiv \delta b_{\rm inst.} \times \delta b_{\rm RMP} \frac{\omega \tau_{\rm v}}{1 + \omega^2 \tau_{\rm v}^2} \qquad (4), \\ F_{\rm B} &\equiv \delta b_{\rm inst.} \times \delta b_{\rm RMP} \frac{\omega \tau_{\rm v}}{\sqrt{1 + \omega^2 \tau_{\rm v}^2}} \qquad (5). \end{split}$$

Here, δb_{RMP} denotes the external coil field.

In conventional models, as illustrated in the conceptual diagram of Fig. 3, an increase in the magnetic fluctuation amplitude leads to a larger braking force, resulting in the frequency approaching nearly zero. Therefore, the observation in LHD, where the post-decrease frequency remains about half of the pre-decrease value, cannot be reproduced. Here, in contrast to conventional models that assume the magnetic fluctuation frequency coincides with the plasma flow (ω_{plasma}), the plasma flow is considered to be shifted by a certain frequency relative to the magnetic fluctuation frequency. The magnetic fluctuation frequency is defined as follows:

$$\omega = \omega_{\text{plasma}} + \omega_{\text{shift}}$$
 (6).

Here, the value of ω_{shift} corresponds to the measured frequency after the decrease. Thus, even when the plasma flow vanishes with increasing magnetic fluctuation amplitude, the magnetic fluctuation frequency can remain finite owing to the frequency shift.

In the discharge shown in Fig. 4, since the external RMP is static, the relative velocity is determined approximately by the magnetic fluctuation frequency. During the acceleration phase, the frequency is low, making it reasonable to apply the no-slip condition, whereas during the deceleration phase, the frequency is high, making it reasonable to apply the slip condition. Each model is illustrated in Fig. 4. It is noteworthy that the same parameters, f_0 and τ_v , are employed for both the deceleration and acceleration phases, and that the value of τ_v is 5 ms, which is comparable to the typical wall time constant evaluated in LHD. Both the gradual frequency variation observed in the deceleration phase and the abrupt frequency increase observed in the acceleration phase are well

IAEA-CN-316/INDICO ID 2698

reproduced. These results suggest that the hysteresis behaviour arises from differences in the frequency dependence of the plasma response to the external RMP.

4. CONSIDERATION OF FREQUENCY SHIFT

The reason for the frequency shift is discussed in this session. In the assumption of the extended model, the plasma flow is nearly zero after the frequency-decreasing phase. Figure 5 illustrates (a) volumed-averaged beta value, (b) magnetic fluctuation, (c) amplitude spectrogram of magnetic fluctuation and peak frequency of dominant Fourier component, and (d) the moving-averaged poloidal flow obtained from Doppler reflectometry[10] (red) and peak frequency (black). Considering the poloidal flow measured by Doppler reflectometry as the plasma flow, it is found that its value is close to zero after the magnetic fluctuation frequency decreases. The magnitude of the frequency shift is approximately 600 Hz.

Next, the direction of the frequency shift is considered. Because both the magnetic fluctuation frequency and the plasma flow are directed in the electron diamagnetic direction, and the magnetic fluctuation frequency is larger than the plasma flow, the resulting frequency shift is also in the electron diamagnetic direction. Therefore, considering the electron diamagnetic drift, which depends on the electron pressure gradient, the electron diamagnetic drift of about 200 Hz is roughly consistent with the observed shift. This result is consistent with previous studies on resistive interchange instabilities in LHD, which demonstrated that the magnetic fluctuation frequency agrees well with the sum of the plasma flow and the electron diamagnetic drift flow[11,12].

In NTM discharges of JT-60U, strong flattening of the pressure gradient led to a reduced electron diamagnetic drift, and as a result, its influence was not observed. In contrast, the present study demonstrates that for Edge instabilities, where the impact of the pressure gradient is relatively weak, a finite electron diamagnetic drift remains, thereby leading to the newly identified effect of frequency shift following the frequency decrease. These results suggest that mode locking can be avoided by sustaining the electron diamagnetic drift through appropriate pressure gradient control.

5. SUMMARY

In this study, modelling of the relationship between the amplitude and frequency of magnetic fluctuations driven by MHD instabilities has been carried out. In LHD and JT-60U, it has previously been observed that, prior to mode locking, the amplitude—frequency relationship follows a unique trajectory, which can be reproduced by the force balance model between the electromagnetic braking force and the viscous driving force. In contrast, phenomena have been observed in which the trajectory differs between the frequency-decreasing and frequency-increasing phases, which cannot be explained by the conventional model. By extending the conventional force balance model, these new behaviours have been successfully reproduced.

As shown in Fig. 6, the conventional model considered only a single braking force model (either slip or no-slip) and therefore could not reproduce the hysteresis. In contrast, the extended model successfully reproduces the observed hysteresis by taking into account a combination of the slip and no-slip models. Furthermore, comparison with behaviours of Edge instabilities in LHD, where the effect on the pressure profile is relatively small, has clarified the influence of the electron diamagnetic drift on the force balance model.

ACKNOWLEDGEMENTS

The authors are grateful to the LHD experiment group for their excellent support. This work was supported in part by the National Institute for Fusion Science under Grant No. KLPH004, by JSPS KAKENHI (No. 23K25856), by a dispatch grant from the Future Energy Research Association, and by Tokamak Reactor Plasma Collaborative Research Programme.

REFERENCES

- [1] ITER Physics Expert Group on Disruptions P C and M 1999 Chapter 3: MHD stability, operational limits and disruptions *Nuclear Fusion* **39** 2251–389
- [2] Hender T C, Wesley J C, Bialek J, Bondeson A, Boozer A H, Buttery R J, Garofalo A, Goodman T P, Granetz R S, Gribov Y, Gruber O, Gryaznevich M, Giruzzi G, Günter S, Hayashi N, Helander P, Hegna C C, Howell D F, Humphreys D A, Huysmans G T A, Hyatt A W, Isayama A, Jardin S C, Kawano Y, Kellman A, Kessel C, Koslowski H R, La Haye R J, Lazzaro E, Liu Y Q, Lukash V, Manickam J, Medvedev S, Mertens V, Mirnov S V.,

Nakamura Y, Navratil G, Okabayashi M, Ozeki T, Paccagnella R, Pautasso G, Porcelli F, Pustovitov V D, Riccardo V, Sato M, Sauter O, Schaffer M J, Shimada M, Sonato P, Strait E J, Sugihara M, Takechi M, Turnbull A D, Westerhof E, Whyte D G, Yoshino R and Zohm H 2007 Chapter 3: MHD stability, operational limits and disruptions *Nuclear Fusion* 47 S128–202

- [3] Erckmann V and Gasparino U 1994 Plasma Physics and Controlled Fusion Electron cyclotron resonance heating and current drive in toroidal fusion plasmas vol 36
- [4] Okabayashi M, Zanca P, Strait E J, Garofalo A M, Hanson J M, In Y, La Haye R J, Marrelli L, Martin P, Paccagnella R, Paz-Soldan C, Piovesan P, Piron C, Piron L, Shiraki D and Volpe F A 2017 Avoidance of tearing mode locking with electro-magnetic torque introduced by feedback-based mode rotation control in DIII-D and RFX-mod *Nuclear Fusion* 57 016035
- [5] Takemura Y, Watanabe K Y, Sakakibara S, Ohdachi S, Narushima Y, Ida K and Yoshinuma M 2021 External RMP effect on locked-mode-like instability in helical plasmas *Nuclear Fusion* **61** 026011
- [6] Isayama A, Matsunaga G, Ishii Y, Sakamoto Y, Moriyama S, Kamada Y and Ozeki T 2010 Effect of Magnetic Island Associated with Neoclassical Tearing Modes on Plasma Rotation in JT-60U Plasma and Fusion Research 5 1–6
- [7] Fitzpatrick R 1993 Interaction of tearing modes with external structures in cylindrical geometry (plasma) *Nuclear Fusion* **33** 1049–84
- [8] Matsunaga G, Takechi M, Kurita G, Ozeki T and Kamada Y 2007 Effect of plasma-wall separation on the stability of resistive wall modes in the JT-60U tokamak *Plasma Phys Control Fusion* 49 95–103
- [9] Takemura Y, Watanabe K, Sakakibara S, Ohdachi S, Narushima Y, Tanaka K and Tokuzawa T 2022 Onset of instability with collapse observed in relatively high density and medium beta regions of LHD *Phys Plasmas* 29 092505
- [10] Tokuzawa T, Inagaki S, Ejiri A, Soga R, Yamada I, Kubo S, Yoshinuma M, Ida K, Suzuki C, Tanaka K, Akiyama T, Kasuya N, Itoh K, Watanabe K, Yamada H and Kawahata K 2014 Ka-band microwave frequency comb doppler reflectometer system for the large helical device *Plasma and Fusion Research* 9 1–6
- [11] Takemura Y, Sakakibara S, Watanabe K and Ichiguchi K 2013 Rotation of Interchange Instability in the Large Helical Device *Plasma and Fusion Research* 8 1–6
- [12] Takemura Y, Watanabe K, Sakakibara S, Ohdachi S, Suzuki Y, Ida K, Yoshinuma M, Yamada I and LHD Experiment Group 2018 Comparison of rotation of interchange mode in large helical device plasmas with various ion species *Plasma and Fusion Research* 13

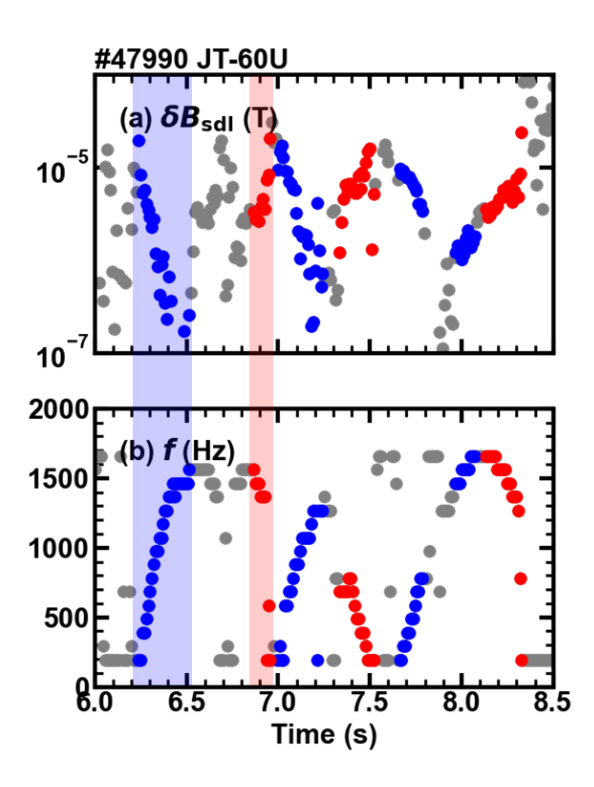


FIG. 1. Time evolution of (a) amplitude and (b) frequency of m/n=2/1 magnetic fluctuation due to NTM in JT-60U. The blue points correspond to the data during the frequency-increasing phase, and the red points correspond to the data during the frequency-decreasing phase.

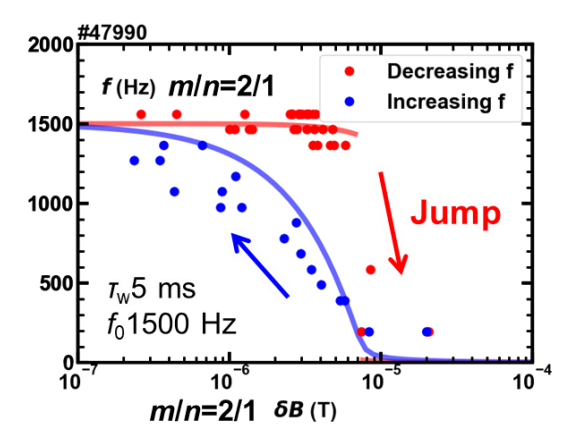


FIG. 2. Hysteresis in the amplitude–frequency trajectory observed in NTM discharge of JT-60U. Red and blue symbols indicate experimental data during frequency decrease and increase, respectively. The no-slip model is represented by the red curve, while the slip model is represented by the blue curve.

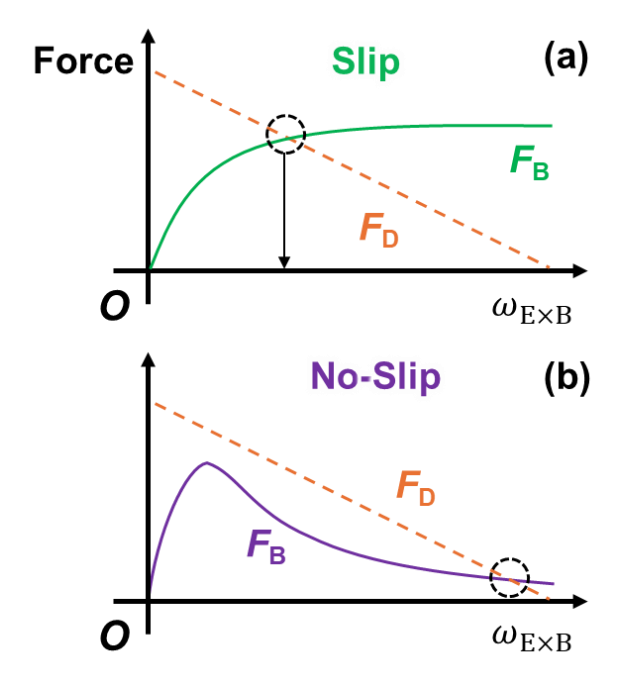


FIG. 3. A conceptual diagram of the force balance model between the braking force F_B and the driving force F_D is shown: (a) the braking and driving forces under the slip condition, while (b) shows those under the no-slip condition. The intersection of the two forces corresponds to the plasma rotation frequency at that time.

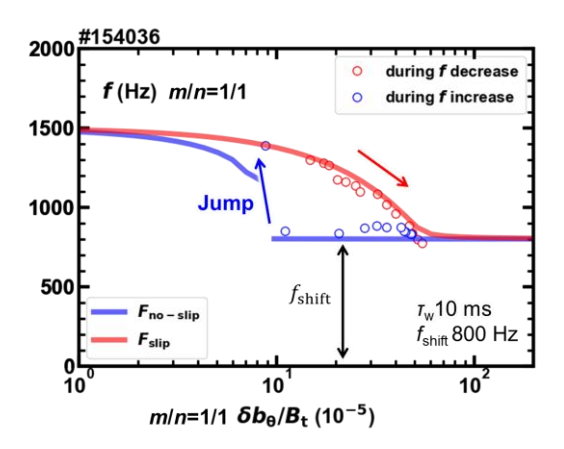


FIG. 4. Hysteresis in the amplitude–frequency trajectory observed in an Edge instability discharge of LHD. Red and blue symbols indicate experimental data during frequency decrease and increase, respectively. The slip model is represented by the red curve, while the no-slip model is represented by the blue curve.

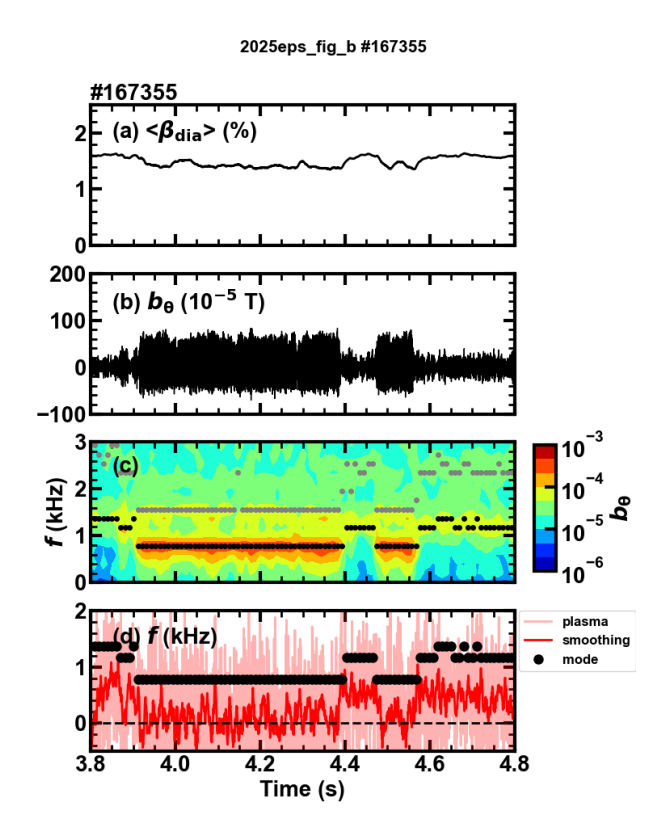


FIG. 5. Poloidal flow measurements in an Edge instability discharge of LHD: (a) volume-averaged beta, (b) magnetic fluctuations, (c) magnetic fluctuation spectrum with spectral peaks indicated by black dots, and (d) comparison of magnetic fluctuation frequency (black dots) with poloidal flow (light red: measured values; dark red: moving average).

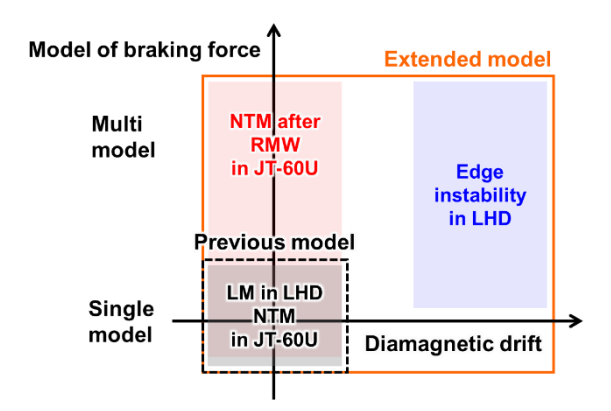


FIG. 6. A conceptual diagram illustrating the parameter space accessible to the extended model. The horizontal axis represents the magnitude of the diamagnetic drift, which is proportional to the pressure gradient during excitation of the instability, while the vertical axis indicates whether the braking force is modelled by a single component or by a combination of multiple components.